Jurnal Teknologi

Full Paper

EFFECT OF STIRRUPS AT BEAM CROSSINGS USING COCOPEAT AS A CONCRETE AGGREGATE SUBSTITUTE FOR SAND

T. Q. K. Lam[a]*, T. A. Le[b]

[a]Faculty of Civil Engineering, Mien Tay Construction University, 85000, Vinh Long, Vietnam
[b]Construction and Network Department, Sai Gon Joint Stock Commercial Bank (SCB), 85000, Vinh Long, Vietnam

Article history
Received
21 October 2024
Received in revised form
25 December 2024
Accepted
31 December 2024
Published Online
22 August 2025

*Corresponding author
Lamkhai@mtu.edu.vn

Graphical abstract

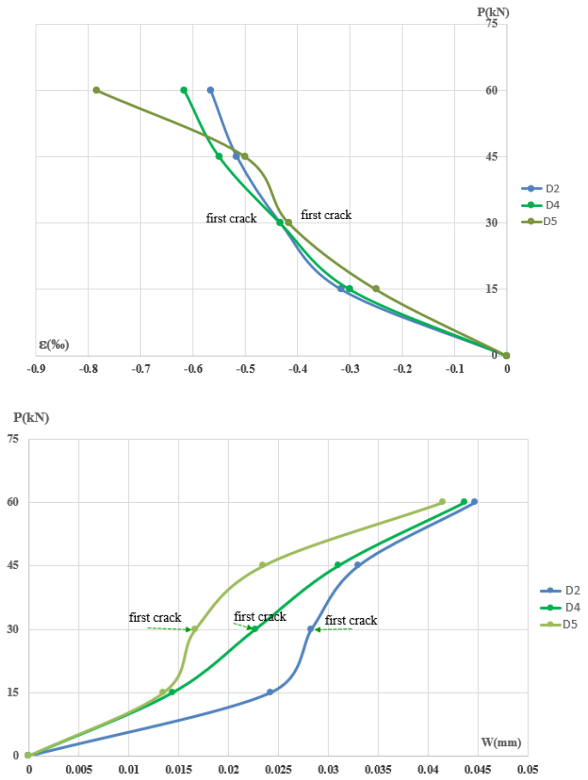

Abstract

Stirrups are included at the intersections of beams, with secondary beams supported by the main beams or positioned where concentrated forces are significant. Additional stirrups must be arranged to enhance the load-bearing capacity at these beam intersections. At these beam intersections, it is necessary to arrange additional stirrups to support the reaction force generated by the secondary beams. At the intersections of the main beams, it is necessary to arrange additional stirrups on the section b+2h (where b and h represent the width and height of the main beam). The use of the stirrup arrangement at the beam intersection, as outlined in the TCVN 5574:2018 standard, has been subject to limited experimental studies. These studies aim to assess whether the stirrup placement at the beam intersection is both reasonable and optimal for ensuring adequate load-bearing capacity in this area. Furthermore, it is essential to investigate the impact of incorporating cocopeat as a partial substitute for sand aggregate in the concrete concerning the performance of these intersecting beams. The research results examined the formation and propagation of cracks, established the relationships between load-vertical displacement and load-compressive (tensile) deformation, explored the impact of additional stirrup arrangements on the behavior of seven experimental reinforced concrete beams, and utilized cocopeat as a sand substitute in concrete with beam dimensions of 0.15×0.2×1.2m.

Keywords: Stirrup, load-bearing capacity, TCVN 5574:2018, cocopeat, aggregate, concrete

1.0 INTRODUCTION

The calculation of stirrups in accordance with the TCVN 5574:2012 standard [1] has proven effective in the arrangement of stirrups at the beam intersection. The calculation of stirrups in this standard is based on Russian standards [2], where the concrete in the compression zone and stirrups are assessed on the inclined section of the beam. Several studies have referenced theoretical calculation methods [3] by examining standards such as TCVN 5574:2012, ACI 318-08 [4], and Eurocode 2 [5]. The experimental method applied to reinforced concrete beam samples [6] compared the arrangement of stirrups at

the beam intersection by varying the stirrup angle to 45^0, 60^0, 75^0, and 90^0 degrees, ultimately identifying the most optimal angle for steel arrangement at the beam intersection. This study found that, in addition to altering the angle of the stirrup, it is also feasible to modify the arrangement of the stirrup at the beam intersection in accordance with the current standard TCVN 5574:2018 [7].

The research examined how the spacing of reinforcement affects the shear capacity of reinforced concrete beams through experimental methods [8]. The research carried out experiments on beams equipped with stirrups under various conditions and showcased the outcomes of 14 compression tests to explore the impact of stirrup spacing on the shear capacity of the beams. The study [3] analyzed and compared the approaches to designing shear stirrups for bending beams according to ACI 318-08 [4], Eurocode 2 [5], and TCVN 5574:2012 [1]. The study revealed that Eurocode 2 [5] overlooked the role of concrete in the shear capacity of reinforced concrete beams, while noting that the crack angle changed based on the load applied. In contrast, TCVN 5574:2012 [1] and ACI 318-08 standards consider the contribution of concrete under shear conditions, although the crack angle remains constant. It is indicated that, of the three standards, utilizing ACI 318-08 [4] is the most straightforward, as the guidelines for executing the calculation steps are clear and uncomplicated. Eurocode 2 [5] is the standard that most effectively demonstrates the behavior of beams under bending and shear forces. At present, TCVN 5574:2012 has been superseded by TCVN 5574:2018 [7]. This new standard shifts the perspective of the calculation model from the stress model to the deformation model. This model is advised for use in calculations pertaining to the first limit state and the second limit state for members experiencing bending moments and axial forces. At the beam intersections, extra horizontal steel should be positioned to support the reaction force generated by the secondary beam. At the intersection position of the main beam, stirrups should be positioned on section b+2h, where b represents the width and h denotes the height of the secondary beam. A section of length equal to h/3 should be arranged at the intersection position of the secondary beam. According to [7], stirrups should be arranged in section (b+2h), with a spacing of 50mm.

The study presents a method for determining the shear stirrups of beams that are subjected to concentrated loads, in accordance with TCVN 5574:2018 [7] of Vietnam, which was established based on the SP 63.13330.2012 [9] standard, along with the guidelines provided in Pocobie for SP 63.13330 [10] of Russia in 2012. Nonetheless, TCVN 5574:2018 of Vietnam does not provide accompanying instructions, leading some authors to investigate and create documents that outline the procedures for calculating shear stirrups for various beams [11–15] in accordance with TCVN 5574:2018 [7]. Indeed, while grounded in the same standard, the calculation outcomes reveal varying approximate and inaccurate results. Based on previous research documents, the authors have synthesized their findings into [16]. This article will present the fundamental theory related to the calculation of shear beam stirrups, outline a practical method for determining the shear capacity of beams, and highlight the shortcomings of this calculation method. The authors subsequently introduced a novel approach for calculating stirrups in beams that are subjected to concentrated loads, in accordance with TCVN 5574:2018. By addressing practical calculation problems aligned with the research directions, the authors' group achieved results indicating that their proposed method aligns effectively with both the design and test problems. This approach ensures safety while also reducing mass in accordance with standard calculations.

Alongside the theoretical calculation research methods, there are also investigations employing experimental techniques. An illustrative case is the investigation of the shear resistance of concrete beams through experimental arrangements of stirrups [6]. This study presents an arrangement of stirrups in the experimental beam structure designed to resist shear force, utilizing a configuration where stirrups are positioned perpendicular to the inclined cracks, diverging from conventional methods. Following the compression practice, the experimental samples demonstrated that the crack widths were significantly narrower compared to beams reinforced with conventional stirrups. The research method demonstrates the enhanced shear resistance of beams and the practicality of utilizing reinforced concrete beams with stirrups.

The current scarcity of sand in construction is becoming increasingly severe. To solve the situation presented above, the government has established processes to promote the use of construction materials as substitutes for natural sand [17]. This initiative encourages research into sea sand alternatives to effectively meet the demand for sand replacement in ongoing projects. Alongside inorganic sand substitutes, there is a growing focus on identifying sand alternatives that consider environmental protection factors, particularly in relation to the greenhouse effect caused by concrete works. Organic alternative materials will be valued as a solution for solving the problem of raw material scarcity and the growing trend towards lightweight and eco-friendly concrete. Vietnam possesses a significant amount of agricultural waste, and it is essential to focus on the utilization and research aimed at transforming this resource for the construction industry. Recent research has explored the use of popular organic fibers, including flax [18], sisal [19-20], coconut fiber [20-24], and palm [25]. The findings suggest that incorporating natural fibers into concrete can enhance its physical and mechanical properties.

Indeed, research and practical applications of organic substances in product manufacturing have

been conducted in Vietnam. An examples case is the research focused on enhancing concrete through the use of cocopeat [26-27]. This study aimed to examine the compressive strength and water absorption through changing the ratio of the normal fine aggregate, sand, with cocopeat, alongside water and cement. The goal was to produce environmentally friendly concrete samples while adhering to the regulations set forth by Vietnamese standards for self-compacting concrete bricks [28].

This study experimentally examines the impact of stirrups at the beam intersection in accordance with TCVN 5574:2018. It also explores the effects of using cocopeat as a substitute for sand aggregate in concrete. The research establishes the relationship between load and compressive (tensile) deformation, as well as the relationship between load and vertical displacement. Additionally, it investigates the formation and propagation of cracks in reinforced concrete beams that use cocopeat as a substitute for sand aggregate, particularly focusing on the bending behavior at the beam intersection.

2.0 METHODOLOGY

2.1 Design of experimental reinforced concrete beams and the use of cocopeat composition as a substitute for sand

This research involved the design of seven reinforced concrete beams. Details of the beams are presented in Figure 1:

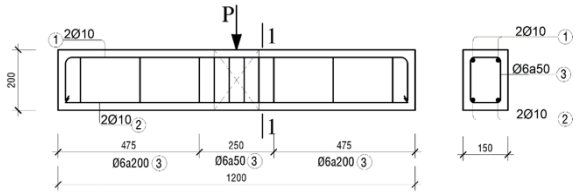

a) D1, Cocopeat content substitutes sand, 0%

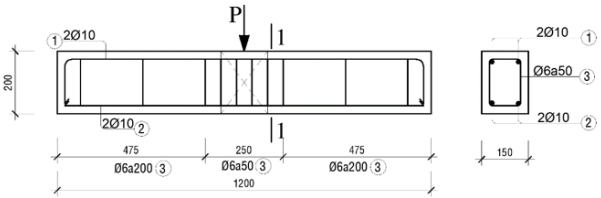

b) D2, Cocopeat content substitutes sand, 20%

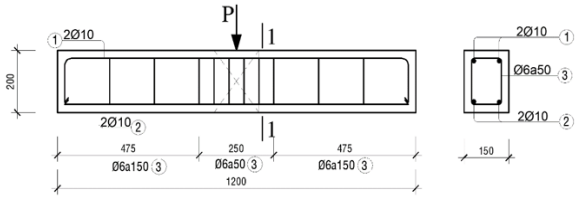

c) D3, Cocopeat content substitutes sand, 20%

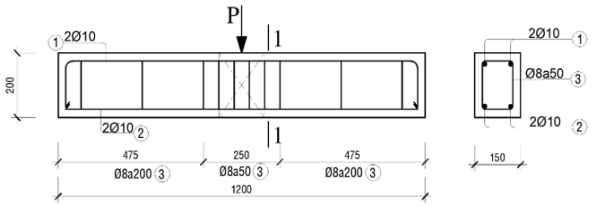

d) D4, Cocopeat content substitutes sand, 20%

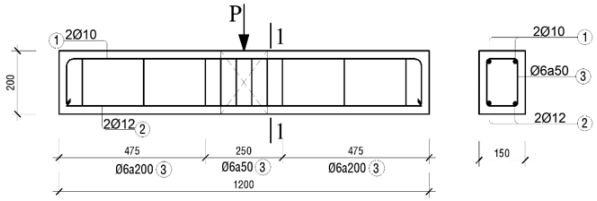

e) D5, Cocopeat content substitutes sand, 20%

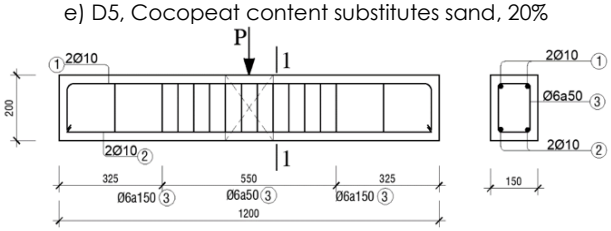

f) D6, Cocopeat content substitutes sand, 20%

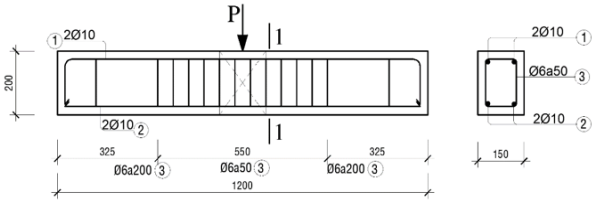

g) D7, Cocopeat content substitutes sand, 20%

Figure 1 Experimental beam model

2.2 Producing cocopeat as a substitute for sand aggregate in concrete

Cocopeat is obtained from the supplier and is then sieved using an appropriate sieve size to remove impurities and fibers mixed with the cocopeat. Once the cocopeat is prepared for testing, it is further dried in the sun to achieve dry cocopeat.

The cocopeat is then moistened carefully. The moisture content is established by determining the quantities of cement and water required to fully hydrate the cement. After numerous trials with varying cement amounts, it has been established that 100g of cocopeat requires 500g of cement for complete coverage on the outside. Following treatment with cement, the cocopeat will be dried in a dry and airy environment for 24 hours. This process aims to allow the cement on the outside of the cocopeat to react with the water absorbed within, resulting in the formation of a hard crystal that is insoluble in water (Figure 2).

Figure 2 Cocopeat after being "hardened" with cement

After sieving to eliminate coconut fiber, the density of cocopeat particles is shown in Table 1.

Table 1 The density of cocopeat particles

Particle size (mm)	density (g/cm³)
0.01 ÷ 0.46	1.15 ÷ 1.46
0.1 ÷ 0.45	1.30 ÷ 1.50
0.2 ÷ 0.25	1.20 ÷ 1.30

2.3 Construction of reinforced concrete beams

The procedure for the manufacture of reinforced concrete beams consists of two primary steps: creating formwork (Figure 3) and pouring concrete (Figure 4). The concrete used is of grade B15, according to TCVN 5574:2018 [7].

Figure 3 The formwork and reinforcement for the beams

Figure 4 Pouring concrete beams

3.0 RESULTS AND DISCUSSION

The beams were installed with devices to determine deformation in the tension and compression regions (both the front and back of the beam), as well as to measure vertical displacement, among other variables under the compressive load of a load cell.

3.1 Formation and propagation of cracks in beams The front surface of beams (shown in Figure 5)

Cracks were observed in beams D1 to D6 at a load level of 30kN (600psi), whereas beam D7 exhibited the first crack at a load level of 15kN (300psi). Both beams D1 and D6 ultimately failed at a load level of 75kN (1500psi). Research on experimental beams revealed that the formation and propagation of cracks in the beams aligned with results from [6] and [8]. The experimental results indicated that the cracks were inclined at an angle of 45 degrees at the midpoint between the beam and the support, with vertical crack development occurring near the center of the beam.

Beam D1 is a normal reinforced concrete beam (0% cocopeat content replacing sand aggregate), with a load-bearing capacity of 75kN. When 20% of the sand aggregate is replaced with cocopeat, the load-bearing capacity of the beams decreases to 60kN (1200psi). Cocopeat is an organic material that is highly porous and lightweight. When covered by an outer layer of cement, it retains internal space, meaning that when incorporated into concrete, it does not achieve the same solidity as normal concrete. This results in a reduced bearing capacity, a typical mechanical property associated with this type of material.

Beam D6, that includes 20% cocopeat content as a substitute of sand aggregate and includes additional stirrups at section b+2h, demonstrates an increase in load-bearing capacity, matching that of beam D1, which contains 0% cocopeat content. Both beams fail at the same load level of 75kN.

a) D1 beam

b) D2 beam

c) D3 beam

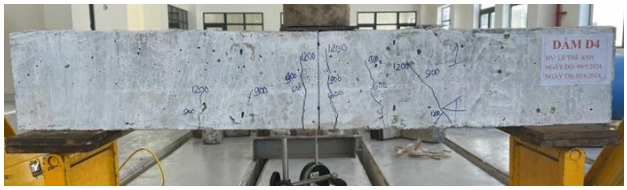

d) D4 beam

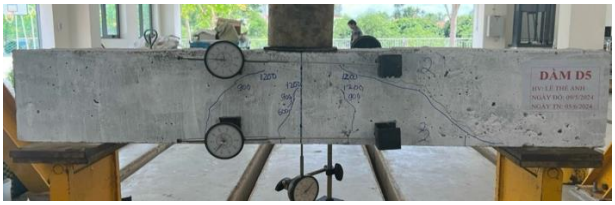

e) D5 beam

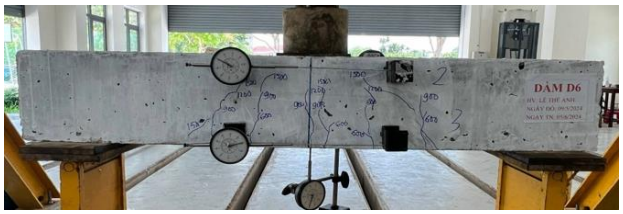

f) D6 beam

g) D7 beam

Figure 5. The front surface of beams

3.2 Load and deformation relationship in reinforced concrete beams

3.2.1 Compressive deformation

Beam D1 and D2: Beam D2 includes 20% cocopeat instead of sand, which causes it to deform more than the normal concrete beam D1 does. This is because the bonding and adhesion between the particles causes major deformation when the beam is under compressive stress. At a load level of 30kN, the difference in deformation is most significant, reaching 73%. Upon reaching a load level of 60kN, beam D2, that includes a cocopeat component, fails, whereas beam D1, constructed with normal concrete, continues to deform up to a load value of 75kN (Figure 6).

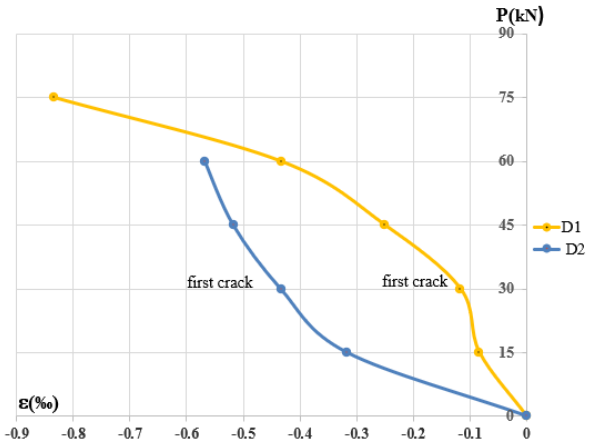

Figure 6. Load-compressive strain of beams D1 and D2

Beam D2 and D3: Both contain 20% cocopeat content substituting sand aggregate in concrete, yet they differ in reinforcement arrangement, resulting in varying compressive strain values for each beam. At a load level of 15kN, beam D2 exhibits a value that surpasses that of D3 by 46%. Upon reaching a load level of 30kN, where the first crack emerges, both beams D2 and D3 exhibit very similar strains, ultimately resulting in identical strain values. This involves to the impact of stirrups when the load reaches a significant magnitude. At a load level of 60kN, where both beams fail, the strain in beam D2 is less than that in D3, with the difference in strain being the most significant at 56% (Figure 7).

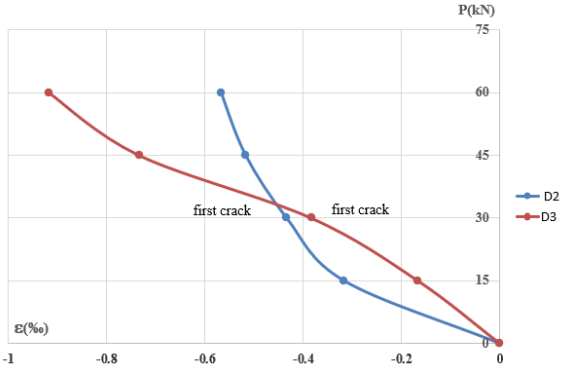

Figure 7 Load-compressive strain of beams D2 and D3

Beam D2 and D4: the compressive strain of both beams has almost the same value (Figure 8). The increase stirrups diameter has no effect on force and slightly change strain at the end.

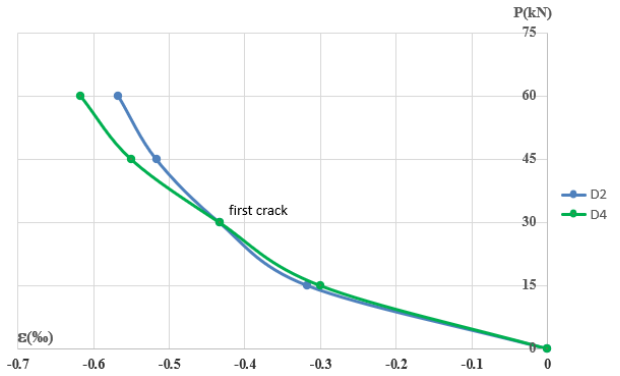

Figure 8 Load-compressive strain of beams D2 and D4

The deformities of the D2 and D5 beams are nearly the same from the beginning of loading up to a 45 kN load. In the experiment, the difference was observed when the longitudinal rebars were changed from ϕ10 to ϕ12 (which indicates a minimal rise in steel content). This change occurred in the tensile zone and happened when the load levels were relatively low. Both beams D2 and D5 showed cracks and had deformation values of 0.42 ‰ and 0.44 ‰, respectively, when the load reached around 30 kN. As the load was increased above 45 kN, the compressive deformation became progressively significant, and both were destroyed at 60 kN. This occurred before the load was increased further. (Figure 9).

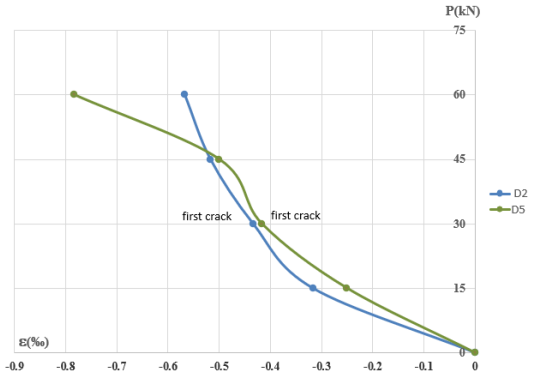

Figure 9 Load-compressive strain of beams D2 and D5

The compressed deformation value of the D6 and D7 beams is nearly identical. At a load of 15 kN, the D7 beam exhibits the first crack and reaches a deformation value of approximately 0.23 ‰. In contrast, the D6 beam shows its first crack at a load of 30 kN, achieving a deformation of 0.39 ‰, indicating that the D6 has a noticeable trace. The crack of D6 is double that of D7. Upon reaching a load of 60 kN, both beams exhibit an equal deformation of 0.63 ‰. However, the D7 beam fails at this point, while the D6 beam remains capable of withstanding an additional load of 75 kN before failure occurs (Figure 10).

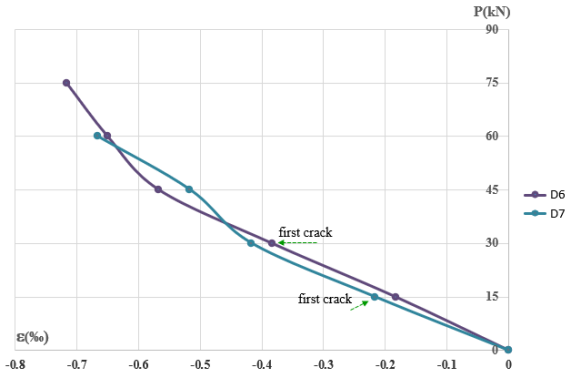

Figure 10 Load-compressive strain of beams D6 and D7

The D2, D4, and D5 beams each contain 20% cocopeat content as a substitute for sand aggregate in the concrete. All three beams exhibit nearly identical compressive deformation when subjected to loads ranging from 0 kN to 45 kN. At the 30kN loading location, all three beams exhibit the first crack, with their deformation values ranging from 0.42 ‰ to 0.44 ‰. All three beams fail under a 60kN load. The deformation at the D5 beam is greater than that of D2 by 28%, while D4 shows a 23% deformation. Additionally, the D4 beam is 5% larger than D2 (Figure 11).

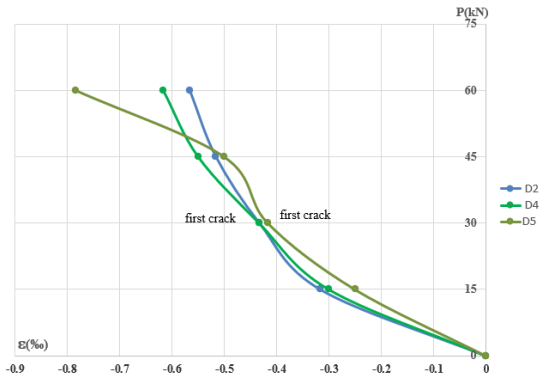

Figure 11 Load-compressive strain of beams D2, D4 and D5

3.2.2 *Tensile deformation*

D1 beams and D2: When subjected to a 15 kN load, the deformation of D2 beams is 68% greater than that of D1 beams. Subsequently, at a loading of 45kN, both beams exhibited a deformation of 1 ‰. At a 60 kN load, D2 experiences a deformation of 1.51 ‰, which is less than D1's deformation of 2.41 ‰. However, D2 ultimately fails, while D1 can endure up to 75 kN before failure occurs (Figure 12).

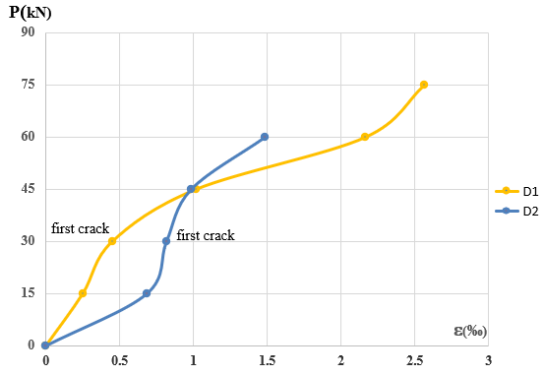

Figure 12 Load-tensile deformation of beams D1 and D2

The results of the compression (Figure 6) and tensile (Figure 12) deformation tests on beams D1 and D2 show that the deformation of beam D2 at the failure position in the compression zone is 0.6‰, whereas the deformation of the tensile zone at the failure position of beam D2 is 1.5‰. This indicates that the deformation of the tensile zone is 2.5 times greater than that of the compression zone. In a way similar to beam D1, the compressive deformation at the failure position has been measured at 0.84‰, whereas the tensile deformation at the same position for beam D1 stands at 2.6‰. This indicates that the deformation in the tensile zone is three times greater than that in the compression zone. This indicates that in beams D1 and D2, the tensile zone exhibits superior load-bearing capacity compared to the compression zone. Additional reason is due to the presence of longitudinal rebars having higher strain capacity and holding the cracks propagation after first crack.

Before cracks developed in the beams, the tensile strain of beam D2 was 18% greater than that of D3. Both beams sustain damage at a load level of 60kN, with the tensile deformation of beam D2 being 27% greater than that of D3 before failure (Figure 13).

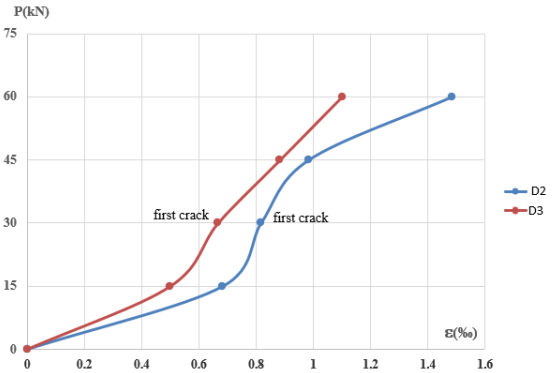

Figure 13 Load-tensile deformation of beams D2 and D3

The experimental results of the deformation in the compression zone (Figure 7) and tension zone (Figure 13) of beam D3 indicate that at the failure load level, the deformation in the compression zone reached 0.92‰, while the deformation in the tension zone at the failure position was 1.1‰. This indicates that the tensile strain is 1.2 times greater than the compressive strain. It suggests the load-bearing capacity of beam D3 in the tensile zone exceeds that of the compressive zone.

The deformation in the tension zone of beams D2 and D4 is consistent across the various load levels. Before cracks developed in the beams, the tensile strain of beam D2 was 54% greater than that of D4. Both beams sustained damage at a load level of 60kN at the same position, exhibiting a deformation of 1.5‰ (Figure 14).

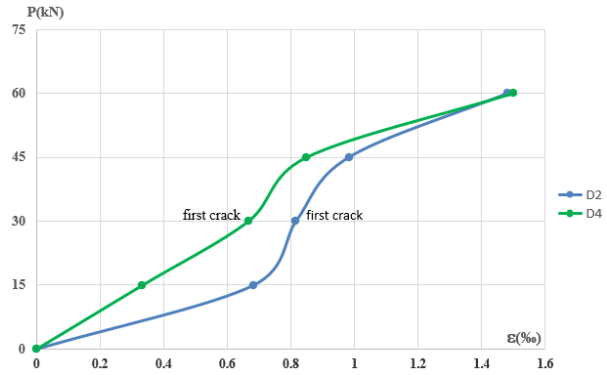

Figure 14 Load-tensile deformation of beams D2 and D4

The results of the compression zone deformation test (Figure 8) and the tensile zone deformation (Figure 14) of beam D4 indicate that the deformation at the failure position in the compression zone reaches 0.62‰, while the tensile zone deformation at the failure position of beam D4 reaches 1.5‰. This indicates that the tensile zone deformation is 2.4 times larger than the compression zone deformation.

Beam D2 and D5: The deformation observed in the tensile zone of the two beams indicates that both straight lines show comparable deformations across the various load levels. Nonetheless, regarding value, beam D2 exhibits greater deformation compared to beam D5. At the 15kN position, beam D2 exhibits a deformation that is approximately 57% greater than that of D5. Additionally, at the load of 30kN, where the crack appears beam D2 is around 37% larger than D5. Both beams showed relatively stable deformation and sustained damage at a load level of 60kN. At the same position, the deformation of beam D2 was approximately 35% greater than that of D5 (Figure 15).

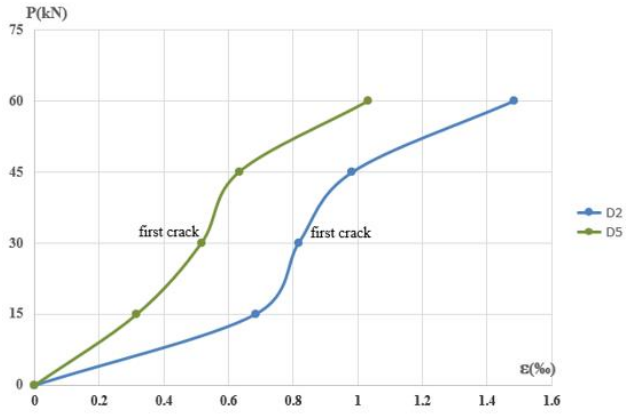

Figure 15 Load-tensile deformation of beams D2 and D5

The results of the compression zone deformation test (Figure 9) and the tensile zone deformation (Figure 15) of beam D5 indicate that the deformation at the failure position in the compression zone reaches approximately 0.8‰, while the tensile zone deformation at the failure position of beam D5 reaches 1‰. This indicates that the tensile zone deformation is approximately 1.25 times greater than the compressive zone deformation. This indicates that the load-bearing capacity of the tensile zone in beam D5 exceeds that of the compressive zone.

Beam D6 and D7: The deformation diagram of the tensile zone for the two beam samples shows similar shapes; however, at various load levels, each beam sample provides different evaluation numbers. When the load ranges from 0kN to 45kN, both beams D6 and D7 show identical tensile zone load-bearing capacities. At a load of 60kN, beam D7 shows a deformation that is approximately 29% greater than that of D6 (Figure 16).

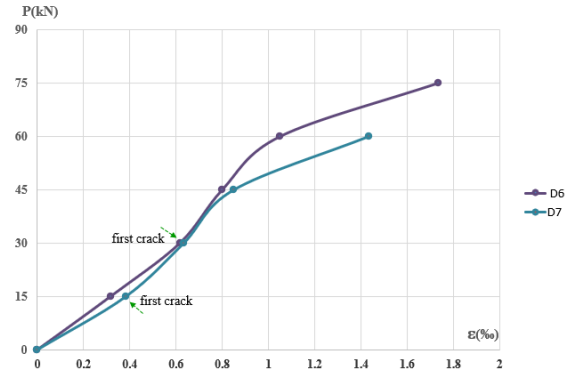

Figure 16 Load-tensile deformation of beams D6 and D7

The results of the compression (Figure 10) and tensile (Figure 16) deformation tests on beams D6 and D7 indicate that the deformation of beam D6 in the compression zone is 0.71‰, whereas the tensile deformation of beam D6 is 1.7‰. This indicates that the tensile deformation is 2.4 times greater than that of the compression zone. In the same way, beam D7 shows a compressive deformation of 0.68‰, whereas its tensile deformation measures 1.42‰, indicating that the tensile deformation is twice as large as the compressive deformation. This indicates that in beams D6 and D7, the load-bearing capacity of the tensile zone exceeds that of the compression zone.

The tensile deformation of beams D2, D4, and D5 is represented by three straight lines that show similarity from the start of loading until failure. At a load level of 15 kN, beam D2 exhibits the greatest deformation in comparison to D4 and D5, which show a deformation of 57%. In the range from 15kN to 45kN, all three beams exhibit comparable deformations. Each beam fails in the tensile zone when the load level hits 60kN. Notably, beam D5 shows less deformation compared to D2, while D4 experiences the same failure rate of 34% (Figure 17).

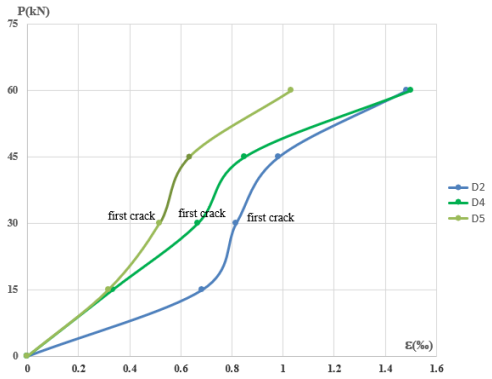

Figure 17 Load-tensile deformation of beams D2, D4 and D5

3.3 Load and vertical displacement relationship at mid-span in beams

Beam D1 and D2: When subjected to a load of 15kN, the mid-span displacement of beam D2 is four times greater than that of beam D1. At the 30kN load level, both beams show cracks, and the displacement of D2 is 2.5 times greater than that of D1. At the 45kN load level, the vertical displacement of D2 shows improvement, yet it remains twice as large as that of D1. At the 60kN load level, beam D2 exhibits a displacement before failure that is 1.8 times greater than that of D1, while D1 is able of withstanding a load of 75kN before failure. The results of the test measuring the vertical displacement between beams indicate that beam D2 exhibits a vertical displacement 2.5 times greater than that of beam D1. In general, it perhaps due to the decrease of concrete strength in D2 (Figure 18).

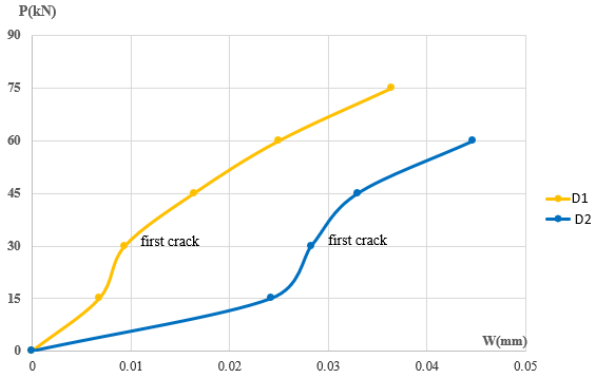

Figure 18 Load-displacement of beams D1 and D2

Beam D2 and D3: When subjected to a load of 15kN, the vertical displacement at mid-span of beam D2 is twice that of beam D3, which also corresponds to the point of maximum vertical displacement. At a load level of 30kN, both beams exhibit cracks, and the vertical displacement of D2 is 1.2 times greater than that of D3. Between the load level of 45kN and the time of failure at 60kN, it is evident that the vertical displacement of D2 has shown improvement in comparison to D3. The experimental results indicate that the vertical displacement at the center of beam D2 is greater than that of beam D3 (Figure 19).

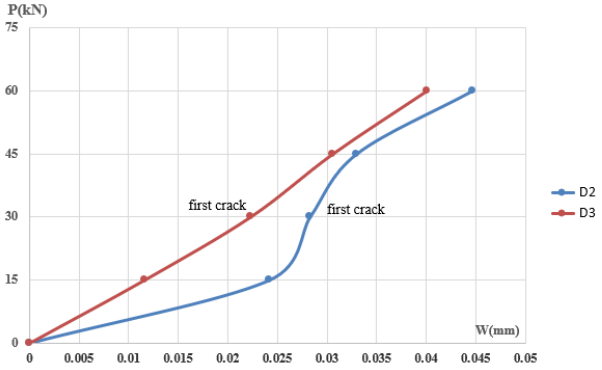

Figure 19 Load-displacement beams D2 and D3

Beam D2 and D4: When subjected to a load of 15 kN, the vertical displacement at mid-span of beam D2 is 1.6 times greater than that of beam D4, which also occurs at the point of maximum vertical displacement. At the load level of 30 kN, both beams exhibit cracks, and the vertical displacement of D2 is 1.2 times greater than that of D4. As the load continues in rising following the cracking of the beams, the vertical displacements at the mid-span of the beams tend to converge closely. (Figure 20).

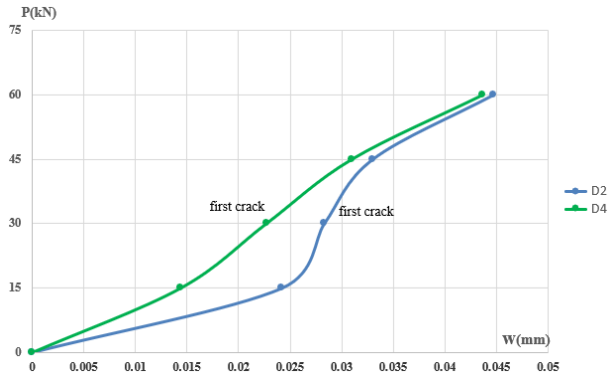

Figure 20 Load-displacement of beams D2 and D4

Beam D2 and D5: When subjected to a load of 15kN, the vertical displacement at mid-span of beam D2 is 1.6 times greater than that of beam D5. At the 30kN load level, both beams exhibit cracks, and the vertical displacement of D2 is 1.8 times greater than that of D5. At the 45kN load level, the vertical displacement of D2 is 1.3 times greater than that of D5. At the 60kN load level, it is observed that the vertical displacement of D2 has shown improvement in comparison to D5 when damaged. The experimental results indicate that the vertical displacement measured between the beams shows beam D2 exhibiting a greater vertical displacement compared to beam D5 (Figure 21).

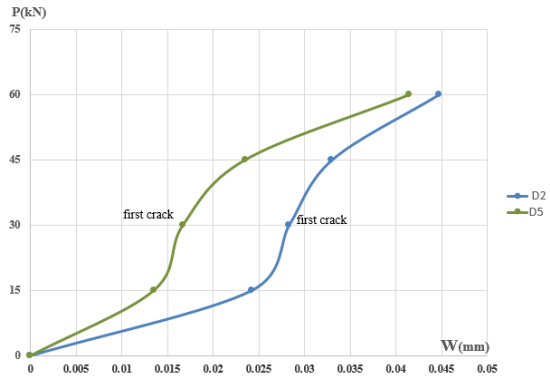

Figure 21 Load-displacement of beams D2 and D5

Beam D6 and D7 exhibit similar vertical displacements within the load range of 0kN to 30kN. However, beam D7 experiences a significant change in vertical displacement starting at a load level of 45kN. At a load level of 60kN, the vertical displacement of beam D7 is 1.4 times greater than that of D6, leading to its failure. Beam D6 continues to support the load up to 75kN before it ultimately fails. The results of the vertical displacement measurement test between beams indicate that beam D7 exhibits a greater vertical displacement compared to beam D6 (Figure 22).

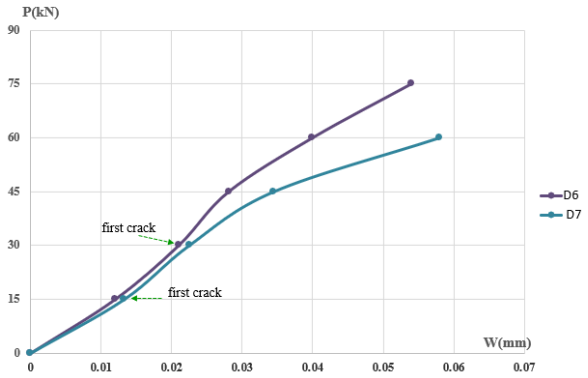

Figure 22 Load-displacement of beams D6 and D7

Beams D2, D4, and D5 show similar vertical displacements. However, within the load range of 15kN to 45kN, the vertical displacements of beams D2 and D5 show unstable variations, in contrast to beam D4, which maintains stable variation across the load levels. For load values below 15kN, there is no difference in the performance of beams D4 and D5 when the rebars are increased from ϕ10 to ϕ12. In beam D2, the influence of the stirrup diameter is clear. As the beams begin to crack, the longitudinal rebars and stirrups have started working (Figure 23).

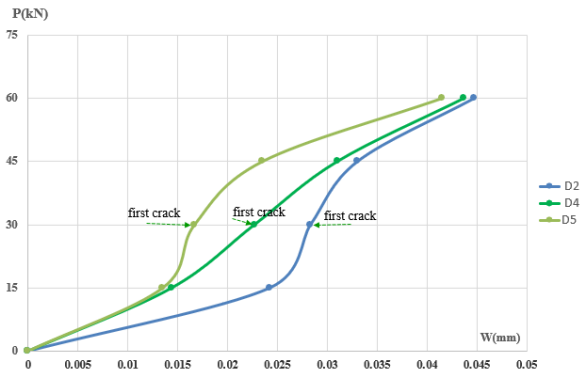

Figure 23 Load-displacement of beams D2, D4 and D5

4.0 CONCLUSION

The study established the relationship between load and vertical displacement of the experimental beams, determining that the load-bearing capacity to failure at mid-span of reinforced concrete beams using cocopeat is 2.5 times smaller than that for normal reinforced concrete beams. Furthermore, the research investigated the formation and propagation of cracks on reinforced concrete beams using 20% cocopeat content treated by the "hardening" method instead of sand aggregate. The results showed that the crack patterns were almost identical to those of normal concrete beams, both in the experiment and in previously published studies. This suggests that reinforced concrete beams with cement-treated cocopeat content can initially perform similarly to conventional ones. In addition, through experimental methods, the author demonstrated the load-bearing capacity of concrete incorporating 20% cocopeat as a sand substitute, indicating its potential for short-term, light-load construction applications. This finding is particularly valuable in the context of current sand resource scarcity. Finally, the research highlights that the bending behavior of reinforced concrete beams is influenced by various factors, including the diameter of the rebars, stirrups, and other structural variables.

Acknowledgement

This study was not funded. The authors declare that there is no conflict of interest regarding the publication of this paper.

Conflicts of Interest

The authors declare that there is no conflict of interest regarding the publication of this paper.

References

[1] Vietnam Standard. 2012. TCVN 5574: 2012. Concrete and Reinforced Concrete Structures - Design Standard.
[2] National Building Code of Russia. 1997. SNiP 2.03.01-84 Concrete and Reinforced Concrete Structures - Design Standards.
[3] P. N. Dung and L. T. T. Ha. 2014. Analysis and Design of Reinforced Concrete Beams Subjected to Bending on Inclined Section according to AIC 318, EUROCODE 2 and TCVN 5575:2012. *Journal of Building Science and Technology*. 3: 63–72.
[4] American Concrete Institute. 2008. ACI 318 – 08. Building Code Requirements for Structural concrete (ACI 318 – 08) and Commentary.
[5] Eurocode 2. 2004. EN1992-1-1. Design of Concrete Structures – Part 1-1: General Rules and Rules for Buildings.
[6] N. B. N. Thao and T. N. Quan. 2021. Experimental Study on Improving Shear Capacity of Reinforced Concrete Beam by Inclined Stirrups. *Journal of science of Lac Hong University*. 13: 84–89.
[7] Vietnam Standard. 2018. TCVN 5574: 2018. Design of Concrete and Reinforced Concrete Structures.
[8] F. Autrup, H. B. Joergensen and L. C. Hoàng. 2022. Experimental Investigation of the Influence of Stirrup Spacing on the Shear Capacity of Reinforced Concrete Beams. *Proceedings of the 14th fib International PhD Symposium in Civil Engineering*, Rome-Italy. 49–56.
[9] SP 63.13330. 2012. Concrete and Reinforced Concrete Structures General, Russian Federation Ministry of Regional Development, 2012.
[10] SP 63.13330. 2012. Concrete and Reinforced Concrete Structures.
[11] E. N. Kodysh, N. N. Trekin, I. K. Nikitin and K. E. Sosedov. 2017. Practical Methods and Examples of Calculation of Reinforced Concrete Structures Made of Heavy Concrete according to SP 63.13330, Moscow.
[12] P. Q. Minh, N. T. Phong, N. T. Thang and V. M. Tung. 2021. Reinforced Concrete Structures (Basic Structural

Components) TCVN 5574:2018. Science and Technology Publishing House.
[13] Hanoi University of Civil Engineering. 2021. Instructions for Calculating Reinforced Concrete Structures according to TCVN 5574:2018 Standard. Science and Technology Publishing House.
[14] B. Q. Bao. 2020. Design of Reinforced Concrete Structures according to TCVN 5574:2018. Construction Publishing House.
[15] L. B. Hue. 2018. Recommendation on the Calculation of Stirrup of Reinforced Concrete Beams Subjected to Concentrated Forces Conforming to SP63.13330.2012. 3: 74–78.
[16] L. B. Hue, P. M. Tuan. 2022. A New Method to Design Stirrups of Reinforced Concrete Beams Subjected to Concentrated Loads according to TCVN 5574:2018. *Journal of Science and Technology in Civil Engineering*. 16(3V): 60–73. Doi: 10.31814/stce.huce(nuce)2022-16(3V)-05.
[17] Prime Minister of Vietnam. (2020). Decision No. 1266/QĐ-TTg Approving the Strategy for the Development of Vietnam's Building Materials for the 2021–2030 Period, with Orientations Toward 2050. Effective January 1, 2021. Official Gazette of the Socialist Republic of Vietnam.
[18] C. Baley. 2002. Analysis of the Flax Fibres Tensile Behaviour and Analysis of the Tensile Stiffness Increase. *Composites Part A: Applied Science and Manufacturing*. 33(7): 939–948. Doi: 10.1016/S1359-835X(02)00040-4.
[19] H. Savastano Jr., P. G Warden, R. S. P. Coutts. 2003. Mechanically Pulped Sisal as Reinforcement in Cementitious Matrices. *Cement and Concrete Composites*. 25(3): 311–319. Doi: 10.1016/S0958-9465(02)00055-0.
[20] R. D. T. Filho, K. Scrivener, G.L. England, K. Ghavami, 2000. Durability of Alkali-sensitive Sisal and Coconut Fibres in Cement Mortar Composites. *Cement and Concrete Composites*. 22(2): 127–143. Doi: 10.1016/S0958-9465(99)00039-6.
[21] A. Zaki, O. Fiardi and K. W. Nindhita. 2024. Evaluation of the Addition of Coconut Fiber Variations in Corroded Concrete Mechanical Properties. *E3S Web of Conf*. 559: 04027. Doi: 10.1051/e3sconf/202455904027.
[22] Khai, C. Y., Mohammad N. N., Mohd R., M. L. F., Md Dan, M. F., & Abu Talib, M. K. 2024. The Comparison of Performance of Root Vetiver Grass between Coconut Fiber and Eggshell toward Slope Stabilization. *Journal of Advanced Research in Applied Mechanics*. 125(1): 185–191. Doi: 10.37934/aram.125.1.185191.
[23] Samina. M. K., Ashok R. M., Vijay S. S., Sonal V. S. and Vaibhav V. S. 2024. A Study of the Effect of Coconut Fiber on Reinforced Concrete Beams Subjected to Combined Bending and Shear. *WJAETS*. 13(01): 556–568. Doi: 10.30574/wjaets.2024.13.1.0432.
[24] Lakshmi Kant *et al.* 2024. Enhancement of Mechanical Strength in Lightweight EPS Geopolymer Composites using Coconut Fiber. *Eng. Res. Express*. 6: 035118. Doi: 10.1088/2631-8695/ad6eeb.
[25] A. Kriker, G. Debicki, A. Bali, K. Mouldi and M. Chabannet. 2005. Mechanical Properties of Date Palm Fibres and Concrete Reinforced with Date Palm Fibres in Hot-dry Climate. *Cement and Concrete Composites*. 27(5): 554–564. Doi: 10.1016/j.cemconcomp.2004.09.015.
[26] L. H. V. Thanh, T. C. Y. Nhi, H. T. K. Hue, *et al*. 2020. Improvement of the Permeable Concrete from Cockle, Rice Husk Ash and Coir Pith. *The University of Danang - Journal of Science and Technology*. 18(5.1): 11–15.
[27] N. M. Trieu. 2024. Research on the Method of Hardening Coco Peat Granules to Replace Sand Aggregate in Concrete. *JSTE-MTU*. 10: 64–79.
[28] Vietnam Standard. 1999TCVN 6476:1999. Interlocking concrete bricks. Ministry of Science and Technology.